

1 **Role of surface phosphorus complexes on the oxidation of porous carbons**

2 M. J. Valero-Romero, F. J. García-Mateos, J. Rodríguez-Mirasol*, T. Cordero

3 Universidad de Málaga, Andalucía Tech, Departamento de Ingeniería Química, Campus

4 de Teatinos s/n, 29071 Málaga, España

5 *Corresponding author. E-mail: mirasol@uma.es

6 **Abstract**

7 Chemical activation of olive stone with phosphoric acid produces activated carbons
8 with relatively high content of P surface groups that remain very stable on the carbon
9 surface at relatively high temperatures. Changes in the surface chemistry of a
10 phosphoric acid activated carbon after subjecting it to thermal treatments in oxidizing
11 and inert conditions are studied by temperature-programmed desorption (TPD), X-ray
12 photoelectron spectroscopy (XPS) and adsorption/desorption of NH₃. TPD and XPS
13 results point out that P surface groups preferentially reacts with molecular oxygen, prior
14 to carbon gasification, through the oxidation of C-P bond to form C-O-P ones, which
15 are thermally stable at temperatures lower than 700 °C. At higher temperatures, these C-
16 O-P type surface groups decompose to less oxygenated P groups on the carbon surface
17 (of C-P type) generating CO (and CO₂) in the gas phase. These C-P type surface groups
18 seem to be very reactive and are (re)oxidized upon contact with air, even at room
19 temperature, forming again C-O-P type groups. Thus, the presence of these oxygen-
20 containing P surface groups with an interesting redox functionality of high chemical and
21 thermal stability seems to be responsible of the high oxidation resistance and high
22 oxygen content (once exposed to ambient air) of this type of porous carbons.

23

24 **Keywords:** phosphorus surface groups, carbon inhibition oxidation, surface redox
25 functionality, activated carbon, temperature-programmed desorption, carbon reduction

26 **1. Introduction**

27 Activation of lignocellulosic materials with phosphoric acid is a well-established
28 method for the preparation of activated carbons with a well-developed porous texture
29 with potential uses in catalysis and adsorption applications. Besides, this method allows,
30 depending on the activation conditions, the preparation of activated carbons with a
31 relatively large amount of P surface complexes of very high thermal stability that confer
32 to these carbonaceous solids high surface acidity and oxidation resistance, increasing
33 the possibilities of these materials for applications in catalysis [1-10]. Another
34 advantage is that these carbon materials can be prepared from different carbonaceous
35 precursors, as agricultural wastes, that are abundant, environmentally friendly disposal
36 and its cost decreases associated with activated carbon production. In the present study,
37 olive stone, an important bio-waste of the agro-food industry in Spain, with a
38 production of more than 450,000 tons/year [11], is used as carbon precursor.

39 The studies of phosphoric acid activated carbons by FTIR, XPS and solid-state
40 NMR techniques pointed out that the remaining P over the surface of the carbon,
41 directly generated during the preparation process under specific conditions, is most
42 likely in form of C-O-P and C-P groups [1, 11-14] . However, some discrepancies are
43 found in the literature associated to the chemical stability of the surface P in
44 phosphorus-containing carbons. In a classic paper, Mckee *et al.* [15] suggested that the
45 C-P-O bonds are not very stable at high temperatures. Oh and Rodriguez proposed an
46 alternative configuration of these C-P-O bonds based on the formation of $p\pi-d\pi$ bond
47 by overlapping p orbitals between P and O. They suggested that this type of bonding in
48 which P=O groups is replacing two edge carbon atoms would be thermally stable to
49 high temperatures [16]. Lee and Radovic [17] showed that the structure with C-O-P
50 bonding is more stable and able to survive longer than the structure with C-P-O

51 bonding, using quantum mechanical modelling. This was later supported by Puziy *et al.*
52 [12, 13] based on IR, XPS and P-NMR methods, since high thermal treated carbons
53 revealed a high contribution of condensed phosphates attached by C-O-P linkage to
54 carbon matrix. Nevertheless, Wu and Radovic proposed later that the O-P bond in the
55 C-O-P system is the weakest one based on ab initio molecular orbital calculations [14].
56 They concluded that when the treatment temperature is increased to high temperatures,
57 the formation of C-PO₃ groups, probably, from decomposition of C-O-PO₃ ones seems
58 to take place. Besides, the ab initio results showed that the C-P bond might be more
59 stable than the C-O-P ones. On this question, Rosas *et al.* [7] observed the release of CO
60 at high temperatures for phosphoric acid activated carbons during a TPD and this
61 behavior was ascribed to the presence of C-O-PO₃ groups on the carbon surface at high
62 temperatures that decompose to C-PO₃ ones.

63 The nature and concentration of these phosphorus functional groups on the surface
64 of the carbon material has a significant influence on the catalyst performance, since this
65 groups act as anchoring sites for the active phase in the preparation of supported
66 catalysts or they can even be the active sites for specific catalytic reactions. In fact,
67 activated carbons prepared by chemical activation using phosphoric acid have been
68 successfully used as acid catalysts in alcohol dehydration reactions [3, 18] and for the
69 decomposition of H₂O₂ [6]. The results reported for alcohols dehydration reactions
70 show that the presence of oxygen in the reaction atmosphere not only leads to a
71 significant enhancement of alcohol conversions, but also inhibits catalyst deactivation
72 and allows steady state conditions to be reached. In addition to its use as solid acid
73 catalyst, redox functionality has been also incorporated by impregnation of these
74 phosphorus containing activated carbons with vanadium species, obtaining a
75 bifunctional catalyst that is active for hydrocarbon partial oxidation reactions [4, 10].

76 The use of phosphoric acid activated carbons as catalysts supports for the selective
77 oxidation of benzene, toluene, and xylene (BTX) [2] has also been reported. Oxygen
78 plays a key role not only in all these catalytic processes, but also in the catalyst
79 performance, since the carbon surface chemistry is modified during the reactions
80 involving oxidizing conditions. Recent investigations have also showed that the
81 presence of C-P type phosphorus groups enhances the functionalization of these
82 materials with nitric acid [19]. Therefore, there is a growing interest on these materials
83 in catalysis and the study of the chemical surface modification under oxidative
84 conditions is investigated in the present work.

85 In addition to this, enrichment of surface oxygen groups on phosphoric acid
86 activated carbons has been observed in most of the above mentioned works, despite the
87 carbons were prepared at relatively high temperatures or were treated to high
88 temperatures under inert conditions. In this sense, it would be of interest to study
89 whether surface re-oxidation may take place on this type of activated carbon during
90 different storage conditions. Therefore, the main purpose of the present work is to study
91 the role of the P surface groups on carbon surface oxidation and reduction reactions. For
92 that, an extensive study of the evolution of oxygen and P surface complexes of an
93 activated carbon prepared by activation of olive stone with phosphoric acid before and
94 after thermal treatments in air and inert atmosphere has been carried out using
95 temperature-programmed desorption (TPD) and X-ray photoelectron spectroscopy
96 (XPS). As a baseline, an activated carbon with similar textural characteristics, but
97 without surface P groups, was also prepared by physical activation of olive stone (CO₂
98 partial gasification) at the same temperature.

99 **2. Experimental Section**

100 **2.1. Activated carbons preparation**

101 Two different activated carbons (with and without phosphorous) were prepared
102 through different pathways: chemical activation with phosphoric acid and physical
103 activation by partial gasification with CO₂. Olive stone waste was used as carbonaceous
104 precursor, in both cases. The olive stone waste was cleaned with deionized water, dried
105 at 100 °C and ground with a roller mill to obtain samples of 400–800 µm particle size.
106 For the chemical activation process, the raw material was impregnated with
107 concentrated H₃PO₄ (85 wt. %, Sigma Aldrich) at room temperature, with a weight ratio
108 of 2/1 (H₃PO₄ /olive stone) and dried for 24 h at 60 °C. The impregnated samples were
109 activated at 800 °C under continuous N₂ (purity 99.999%, Air Liquide) flow (150 cm³
110 STP/min) in a conventional tubular furnace. The activation temperature was reached at
111 a heating rate of 10 °C/min and maintained for 2 h. The activated sample was cooled
112 inside the furnace under the same N₂ flow and then washed with distilled water until
113 negative phosphate analysis in the eluate [20]. The resulting activated carbon, denoted
114 by ACP2800, was dried at 60 °C and, then, grinded and sieved (100-300 µm).

115 For the physical activation process, a procedure described previously by our research
116 group was followed [21], in which the gasification conditions, i.e. gasification temperature
117 and reaction time, as well as the particle size, were set in order to warrant chemical reaction
118 control to achieve a carbon burn-off value of around 55 %. An olive stone char was
119 obtained by carbonizing the raw material under N₂ flow at 800 °C. This char was heated
120 under N₂ atmosphere to the gasification temperature (800 °C). Then, the gas feed was
121 switched to CO₂ (99.998 %, Air Liquide) with a flow rate of 150 cm³ STP/min for 7 h. The
122 resulting activated carbon, denoted by ACG800, was washed under stirring at room
123 temperature for 1 h with 1% HCl in order to remove mineral components. ACG800 sample
124 was chemical activated with H₃PO₄ following the same procedure than that performed to
125 prepare ACP2800, resulting in ACG800-P2 carbon.

126 **2.2. Thermogravimetric analysis**

127 Thermogravimetric analysis (TG) were performed in a CI Electronics MK2 balance
128 under air flow ($150 \text{ cm}^3 \text{ STP/min}$) from room temperature to $900 \text{ }^\circ\text{C}$ at a heating rate of
129 $10 \text{ }^\circ\text{C/min}$, with a sample weight of about 20 mg. Simultaneous thermal-gravimetric
130 analysis and differential thermal analysis (TGA/DTA Mettler-Toledo) was used for
131 investigating the re-oxidation process at room temperature after a thermal treatment at
132 $900 \text{ }^\circ\text{C}$. In this way, sample weight variation and heat involved in the process were
133 simultaneously analyzed.

134 **2.3. Porous texture characterization**

135 The porous texture of the samples was characterized by N_2 adsorption–desorption
136 at $-196 \text{ }^\circ\text{C}$ and by CO_2 adsorption at $0 \text{ }^\circ\text{C}$, using an ASAP 2020 apparatus
137 (Micromeritics). Samples were previously out-gassed at 50 torr and $150 \text{ }^\circ\text{C}$ for 8 h.
138 From the N_2 adsorption/desorption isotherm, the apparent surface area (A_{BET}) was
139 determined from the BET equation [22]. The micropore volume (V_{DR}) was obtained by
140 the Dubinin-Radushkevich (DR) method applied to the CO_2 and N_2 adsorption
141 isotherms [23]. The mesopore volume (V_{mes}) was determined as the difference between
142 the adsorbed volume of N_2 at a relative pressure of 0.95 and the micropore volume
143 (V_{DR}), covering only the pore sizes between 2 and 40 nm, according to the Kelvin
144 equation [24].

145 **2.4. Surface chemistry characterization and elemental composition**

146 Ultimate analysis of the carbons was carried out in a Leco CHNS-932 system,
147 being the oxygen content calculated by difference. The total amount of P was analyzed
148 by inductively coupled plasma optical emission spectrometry (ICP-OES).

149 The surface chemistry of the samples was analyzed by X-ray photoelectron
150 spectroscopy (XPS) using a *5700C model Physical Electronics* apparatus with *MgK α*

151 radiation (1253.6 eV). For the analysis of the XPS peaks, the C_{1s} peak position was set
152 at 284.5 eV and used as reference to locate the other peaks position. The deconvolution
153 of the peaks was done using Gaussian-Lorentzian curves and a Shirley type background
154 line.

155 Temperature-programmed desorption (TPD) profiles were obtained in a customized
156 quartz fixed-bed reactor placed inside an electrical furnace and coupled to a mass
157 spectrometer (Pfeiffer Omnistar GSD-301) and to non-dispersive infrared (NDIR) gas
158 analyzers (Siemens ULTRAMAT 22) in order to quantify CO, CO₂, H₂ and H₂O
159 (calibration error < 1%). In these experiments, c.a. 100 mg of the sample was heated
160 from room temperature to 1000 °C at a heating rate of 10 °C/min in nitrogen (purity
161 99.999%, Air Liquide) flow (200 cm³ STP/min). The absence of any leak was carefully
162 checked before each experiment and the samples submitted to this thermal treatment
163 were denoted by -TT.

164 XPS and TPD analysis were also carried out in order to characterize the oxygen
165 surface groups (OSG) of the carbon catalyst generated after oxidations in air (purity
166 99.999%, Air Liquide) at different temperatures. The samples were heated from room
167 temperature up to 120, 180, 240, 325 and 350 °C at a heating rate of 10 °C/min in
168 nitrogen flow (200 cm³ STP/min) that was changed to air at the same flow rate when the
169 chosen temperature was reached and maintained for 2 h. After these 2 hours of
170 experiment, the inlet gas was again changed to nitrogen until all the oxygen was
171 evacuated from the reactor and lines (followed by mass spectroscopy). Finally, a TPD
172 experiment was carried out up to 950 °C in N₂ flow. The samples submitted to air
173 oxidation were denoted by -OT, where T is the air oxidation temperature.

174 Temperature-programmed desorption of ammonia (NH₃-TPD) was performed using
175 100 mg of catalysts saturated with NH₃ (20% vol in Helium) at 100°C. After saturation,

176 the NH₃ weakly adsorbed was desorbed in a He flow at the adsorption temperature, until
 177 no NH₃ was detected in the outlet gas. The TPD was performed by raising the
 178 temperature up to 500 °C at a heating rate of 10 °C/min. Outlet NH₃ concentrations were
 179 measured by mass spectroscopy (Pfeiffer Vacuum, OmniStar model).

180 Uncertainties were calculated using Student's t-values for 95 % confidence
 181 intervals and random standard uncertainties per ASTM method, as detailed elsewhere
 182 [25]. The uncertainties are presented in the tables.

183 3. Results and discussion

184 3.1. Characterization of the activated carbons

185 Table 1 summarizes the yields and the porous texture parameters of the original
 186 activated carbons. The activated carbon obtained by gasification with CO₂, ACG800,
 187 shows very low yield (13.5 ± 0.4 %, after carbonization and partial gasification).
 188 However, the activated carbon prepared by chemical activation with H₃PO₄ at the same
 189 temperature, ACP2800, presents a yield value of 38.7 ± 0.8 %, which is similar to those
 190 obtained under similar conditions with other biomass residues [7, 11, 26]. The
 191 activation agent, H₃PO₄, restricts the formation of tars and volatiles during the
 192 carbonization process, thus increasing the yield of the remaining solid product [27].

193 **Table 1.** Yield and porous textural parameters values of the activated carbons^a.

Sample	Yield	N ₂ isotherm			CO ₂ isotherm	
	(%)	ABET (m ² /g)	V _{DR} (cm ³ /g)	V _{mes} (cm ³ /g)	A _{DR} (m ² /g)	V _{DR} (cm ³ /g)
ACG800	13.5 (0.4)	1355 (7)	0.570 (0.007)	0.064 (0.004)	870 (3)	0.349 (0.005)
ACG800-P2	10.3 (0.2)	1506 (9)	0.591 (0.009)	0.063 (0.004)	940 (4)	0.377 (0.004)
ACP2800	38.7 (0.8)	1380 (7)	0.514 (0.006)	0.654 (0.010)	662 (2)	0.265 (0.003)

194 ^aThe uncertainties are provided in parentheses.

195
 196 Both activated carbons show higher DR micropore volume values when N₂ is used
 197 instead of CO₂ as the adsorbate gas, which indicates the presence of a wide microporous

198 texture [28]. The phosphoric acid activated carbon, ACP2800, presents higher values of
199 BET surface area and mesopore volume, which confirm that activation of olive stone
200 with phosphoric acid produces a significant contribution of mesoporosity. The activated
201 carbon ACG800, obtained by physical activation, presents a similar surface area, but
202 lower volume of mesopores.

203 The elemental composition and characterization of the surface chemistry of the
204 activated carbons are shown in Table 2. The main elements found on the surface of the
205 phosphoric acid activated carbons are carbon and oxygen, with lower, but still
206 significant amount of P. Nitrogen was also detected, but at very low concentrations,
207 probably being a remnant of nitrogen originally present in the carbon precursor.

208 Phosphoric acid appears to activate olive stone through the formation of phosphate and
209 polyphosphate bridges that crosslink biopolymer fragments, avoiding the contraction of
210 the structure by pyrolysis [18]. Most of the activating agent is removed during the
211 washing step, however part of the P is retained in the structure during the activation
212 process and seems to be stably bonded to carbon because they do not elute after the
213 washing step. The maximum amount of P surface groups that are introduced into carbon
214 structure during the activation process is attained at 700-800 °C, according to previous
215 works [11, 18, 29]. The mass surface concentration of P determined by XPS (3.5 wt. %)
216 is very similar to that obtained by ICP-OES (3.7 wt.%) with uncertainties of 0.2 in each
217 case, indicating that P complexes are well distributed overall the carbon particles
218 surface, internal and external. No other inorganic elements were detected on the surface
219 of ACP2800, as they are removed by the phosphoric acid activation treatment. On the
220 other hand, the ACG800 surface is composed mostly by carbon and oxygen and no P
221 was found on it. Other mineral components like sodium, calcium and potassium, which
222 were originally present in the carbon precursor in very low amount, were removed to a

223 large extent after a washing step, being present in quantity lower than 0.5 wt. %. In fact,
 224 the ash content for ACG800 sample is very low, 0.3% (Table 2). In the case of
 225 phosphoric acid activated carbons, the main inorganic constituent of the activated
 226 carbon ashes is phosphorus, in form of P₂O₅, as revealed by XPS analysis (not shown).
 227 **Table 2.** Ash values, elemental composition and surface chemistry characterization (XPS) of
 228 the activated carbons ^a.

Sample	Ash	Elemental Analysis (wt. %)					XPS (wt. %)		
	(wt. %)	C	O (by diff.)	H	N	S	C _{1s}	O _{1s}	P _{2p}
ACG800	0.3 (0.1)	93.2 (0.7)	4.7 (0.2)	1.2 (0.1)	0.5 (0.1)	0.1 (0.1)	97.8 (0.8)	3.2 (0.2)	-
ACG800-P2	3.7 (0.2)	87.9 (0.7)	6.7 (0.2)	1.3 (0.1)	0.4 (0.1)	0.0 (0.1)	90.2 (0.7)	7.3 (0.3)	2.5 (0.1)
ACP2800	6.0 (0.2)	82.4 (0.6)	9.3 (0.3)	1.9 (0.1)	0.4 (0.1)	0.0 (0.1)	87.3 (0.6)	9.2 (0.3)	3.5 (0.2)

229 ^aThe uncertainties are provided in parentheses.

230 A very interesting feature observed here is that ACP2800 carbon contains a
 231 considerable amount of oxygen (9.3 ± 0.3 wt. %), despite having been activated in an
 232 inert atmosphere (N₂). In fact, the oxygen content in phosphoric acid activated carbons
 233 has also shown to reach a maximum for samples activated at 700-800 °C and decreases
 234 at higher temperatures, in parallelism with the P content [11, 18, 29], which might
 235 suggest that incorporation of oxygen to the carbon surface is related to the P surface
 236 content.

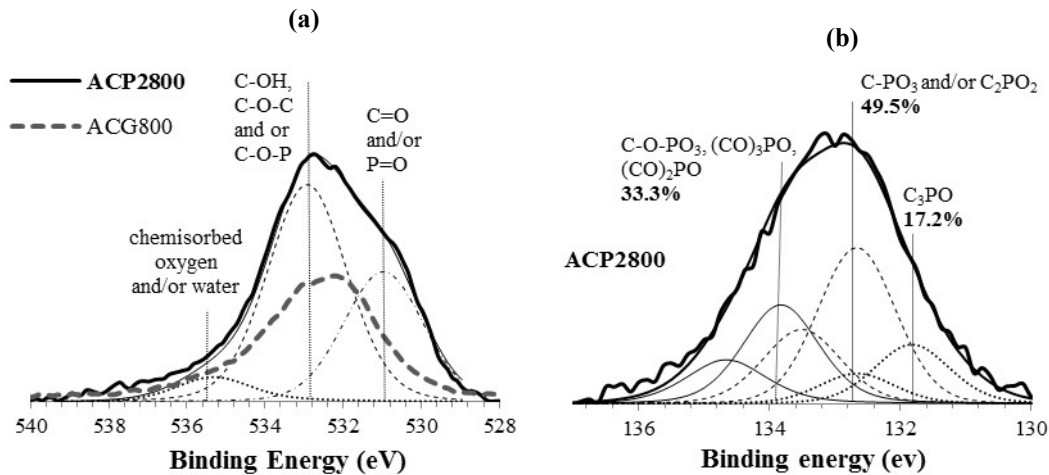
237 Information about the chemical nature of OSG present in the activated carbons is
 238 obtained by analysing the XPS and TPD profiles. Figure S1 shows the C_{1s} spectrum for
 239 ACG800 and ACP2800 showing its deconvolution into six components according to the
 240 analysis of the C_{1s} region of carbon materials reported elsewhere [12, 13, 30]. The BE
 241 of carbon bound to phosphorus (C–P bonding) is between graphitic and aliphatic carbon
 242 bonds and thus cannot be clearly determined [31]. 62 and 15 % of surface carbon atoms
 243 for ACP2800 are graphitic and aliphatic, respectively, whereas those for ACG800 are
 244 66 and 10%. About 20 % belongs to oxidized carbon.

245 The O_{1s} spectrum of ACP2800 sample (Figure 1a) shows a high contribution for
246 oxygen at a binding energy of 532.6 eV, which is characteristic of single bonded
247 oxygen in C-OH, C-O-C and/or C-O-P linkages. Compared to that of ACG800, the O_{1s}
248 spectrum for ACP2800 shows a more pronounced shoulder at lower binding energies,
249 characteristic of C=O and/or P=O groups (BE = 530.9 eV). A binding energy of 535.5
250 eV is related to chemisorbed oxygen and/or water [32].

251 The P_{2p} spectrum for ACP2800 (Figure 1b) shows a band with a main peak at a
252 binding energy of about 133.7 eV, which is characteristic of pentavalent
253 tetracoordinated phosphorus (PO_4) as in phosphates and/or polyphosphates [11, 13].
254 This broad band can be deconvoluted in different doublets with an area ratio of 0.5 and
255 a distance between peaks of 0.84 eV. Wu and Radovic assigned the peak at a binding
256 energy about 134.0 eV to C-O-P type bonds [14], in where the P atom is bonded to four
257 O atoms by one double bond and three single bonds, such as in C-O- PO_3 groups. These
258 authors suggested that these groups could be in the form of numerous cross-linked
259 structures attached to the carbon surface. Thus, $(C-O)_2PO_2$ and/or $(C-O)_3PO$ could also
260 be formed on the surface of the carbon. A binding energy of about 133.2 eV is
261 characteristic of C-P bonding as in C- PO_3 groups [14], where P is bonded to one C and
262 three O atoms (two single and one double bonds), and/or C_2PO_2 . Lower value of
263 binding energies at 132.0 and 131 eV can be associated to C_3PO [14, 33, 34] and C_3P
264 groups [35], respectively. The XPS P_{2p} results for ACP2800 seem to indicate the
265 presence of mainly C- PO_3 (49.5 %) and C-O- PO_3 (33.3 %) type groups on the activated
266 carbon surface.

267

268



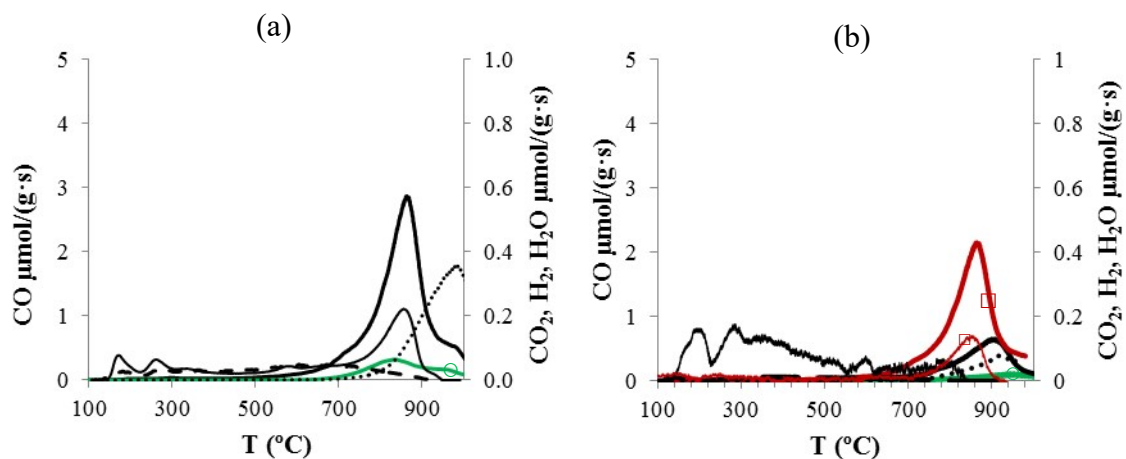
270

271 **Figure 1.** Representative XPS spectra for O_{1s} region of ACG800 and ACP2800 (a) and
 272 for P_{2p} region of ACP2800 (b), showing their deconvolution.

273 Figures 2a and 2b show the evolution of CO, CO₂, H₂O and H₂ as a function of
 274 temperature during the TPD for ACP2800 and ACG800, respectively. In addition, a
 275 second TPD experiment was performed immediately after the first one on the activated
 276 carbons, without exposure to ambient air, in order to elucidate the thermal stability of
 277 the OSG. The CO-TPD profiles during the second TPD run (CO-2nd TPD) are also
 278 presented (green line (—○—)) in Figure 2. Carbon-oxygen groups of acidic character
 279 (carboxylic, lactonic) evolve as CO₂ upon thermal decomposition in a typical TPD
 280 analysis, whereas non-acidic ones (carbonyl, ether, quinone and phenol) evolve as CO.
 281 Anhydride surface groups evolve as both CO and CO₂ [36, 37]. According to previous
 282 studies, phenols evolve as CO between 600-700 °C [36-39], ether groups at around 700
 283 °C, carbonyls between 800-900 °C and more stable chromenes or pyrone groups have
 284 also been reported to evolve as CO at around 1000 °C [40].

285 The TPD profile of ACP2800 (Figure 2a) shows a significant CO evolution at
 286 temperatures higher than 750 °C that presents a maximum at 860 °C, which has been
 287 previously assigned to the decomposition of stable C–O–P type bonds of C–O–PO₃

288 surface groups, producing C'-PO₃ surface groups, where C' here refers to a new surface
 289 carbon atom [8, 14]. On the other hand, the CO₂ profile shows very low desorbed
 290 amount in comparison to that of CO, indicating a lower presence of carboxyl, lactonic
 291 and anhydride groups on this sample. The washing step performed after the chemical
 292 activation process could have introduced some of these OSG of low thermal stability.
 293 The relatively higher amount of CO₂ that evolves at temperatures higher to 750 °C,
 294 associated to the peak of CO at those temperatures, is probably due to decomposition of
 295 stable O=C-O-P surface groups [41], although secondary reactions between the CO
 296 released at these temperatures and the OSG cannot be disregarded [42].
 297



298
 299 **Figure 2.** Amount of CO (1st TPD (—) and 2nd TPD (○—)), CO₂ (—), H₂O (---) and H₂ (.....)
 300 evolved as a function of temperature during the TPD performed to ACP2800 (a) and ACG800
 301 (b). Amount of CO (□—) and CO₂ (□—) during the TPD performed to ACG800-P2 (b).

302 The H₂O profile of the TPD for ACP2800 sample shows a peak with a maximum at
 303 approximately 150 °C that corresponds mainly to physisorbed water, while a second
 304 desorption peak with a maximum at 270 °C can be associated to dehydration of two
 305 neighboring carboxylic groups. The slight H₂O evolution observed up to 800 °C could
 306 be associated to dehydration of P-OH groups, which have been reported to be thermally
 307 stable [43]. In the last case, generation of C-O-PO₂-C and/or C-O-PO(C)₂ type surface

308 groups might occur, if dehydration of one and/or two –OH of the phosphate group takes
309 place, respectively, followed by the breakage of the C–O–P bonds at higher
310 temperatures (from about 750 to 950 °C), forming finally C₃PO type surface groups
311 with new surface carbon atoms and gaseous CO. Similar results have been observed for
312 activated carbons obtained by chemical activation with phosphoric acid of different raw
313 materials [8, 33]. There is also some H₂ release starting at 800 °C, probably as a
314 consequence of aromatic condensation of the carbon substrate.

315 The main peak on the CO profile for ACG800 carbon (Figure 2b) is located at
316 about 900 °C and may be associated to carbonyl/quinone or esthers groups, given that
317 this carbon does not present any P on the surface. Besides, the shoulder at 270 °C and
318 the large tail of the CO₂ profile between 350-650 °C indicate the presence of anhydrides
319 and lactonic groups. The small amount of CO₂ that evolves at temperatures above 800
320 °C is, probably, a result of secondary reactions between the CO and the OSG, as it has
321 been commented previously.

322 The amount of oxygen evolved during the first TPDs for both carbons have been
323 calculated from the total amounts of CO and CO₂ desorbed. The results are 2.6 ± 0.2
324 and 5.4 ± 0.4 wt. % of oxygen for ACG800 and ACP2800, respectively. Comparison of
325 these results with those for the elemental composition, showed in Table 2, indicates that
326 most of the oxygen on sample ACG800 has been desorbed as CO and CO₂ during the
327 first TPD up to 1000 °C. However, ACP2800 shows a small presence of CO at high
328 temperatures (>800 °C) during a second TPD, which can be associated to
329 decomposition of C–O–P type bonds, and almost no evolution of CO₂ (>800 °C), H₂
330 and H₂O (not shown). According to the literature, remaining CO-evolving surface
331 groups of very high thermal stability may show some degree of mobility on the carbon
332 surface [39, 44]. Thus, when the temperature is dropping during the first TPD

333 experiment the oxygen of these CO-evolving groups may migrate to previously
334 generated surface sites of C'-P type, in this case, producing OSG of lower thermal
335 stability that decompose as CO during the second TPD. The amount of CO evolved for
336 the ACP2800 carbon became negligible after a third TPD, indicating that the only
337 oxygen source inside the oven during the thermal treatment of ACP2800 sample must
338 be oxygen evolved from the corresponding OSG.

339 ACG800 carbon was impregnated with H₃PO₄ at an impregnation ratio (mass of H₃PO₄
340 to mass of ACG800) value of 2 and carbonized at 800 °C. After cooling down to room
341 temperature, this sample was washed at the same conditions as ACP2800 was prepared.
342 The new sample thus prepared was denoted by ACG800-P2 and their textural and
343 surface chemistry characteristics are shown in Table 1 and 2, respectively. It is
344 interesting to point out that this sample present 2.5 ± 0.1 wt. % surface P, as measured
345 by XPS (Table 2). The P_{2p} region of the XPS spectrum of ACG800-P2 (not shown) is
346 very similar to that of ACP2800, indicating that ACG800-P2 presents the same P
347 surface complexes as ACP2800. Also, the TPD profile for ACG800-P2 shows a large
348 evolution of CO (and CO₂) at high temperatures (Fig. 2 b, red line (-□-)), with a peak
349 centered at 860 °C, not observed in the TPD profile of ACG800. These experimental
350 evidences support the hypothesis previously exposed that the CO evolved at high
351 temperatures (at about 860 °C) for samples containing P surface groups result from the
352 decomposition of these P surface complexes.

353 **3.2. Oxidation of activated carbons**

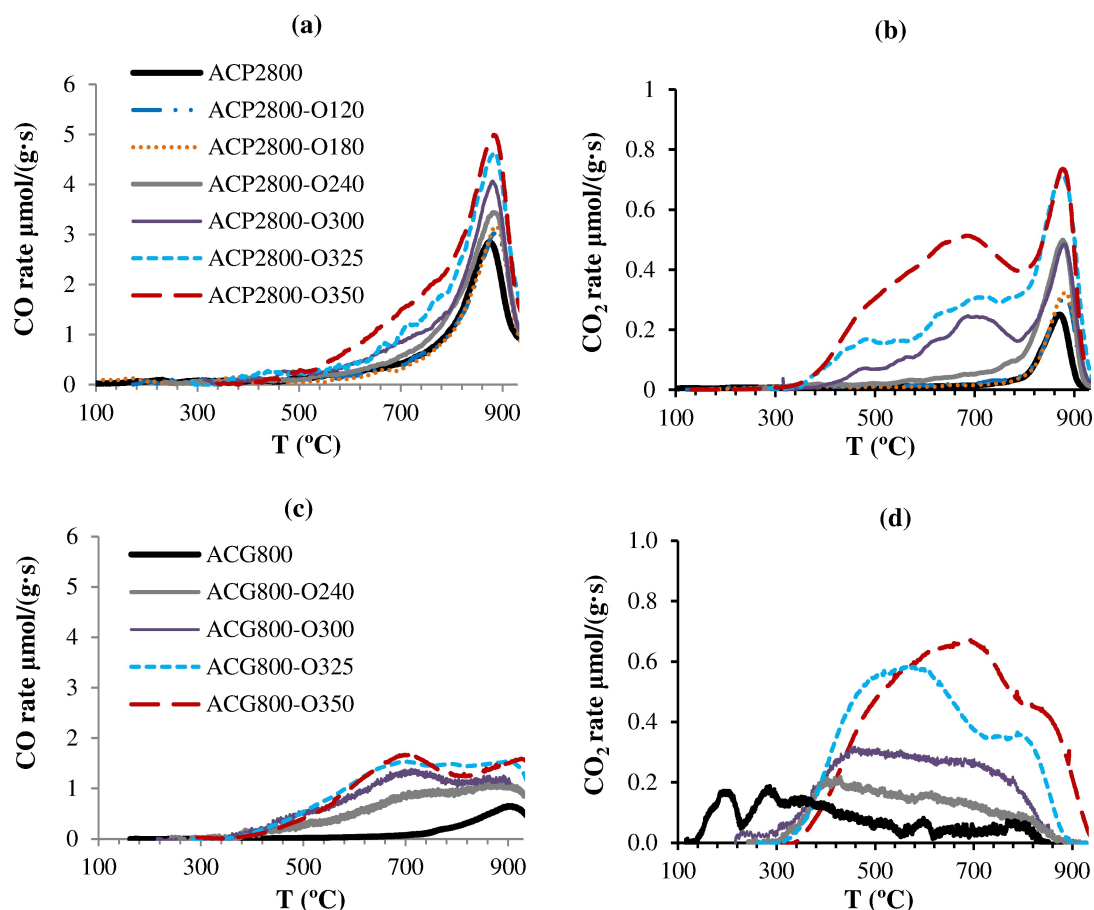
354 The interest on improving the oxidation resistance of carbon materials by
355 introduction of different kinds of surface dopants (especially B and P) is clear from the
356 large number of research papers on this subject. Nevertheless, this is a matter under

357 continuous discussion due to their inherent complexity. P shows an important oxidation
358 inhibition effect, observed in carbon treated with different P compounds, such as
359 organo-phosphorus compounds [17], POCl_3 [45] or H_3PO_4 [41, 45, 46]. We should
360 emphasize here that in our case the surface P groups are directly generated during the
361 carbon preparation process under specific conditions and seem to be strongly bonded to
362 the carbon surface and thermally very stable. The P surface complexes could be
363 probably located at the edges of carbon crystallites, stabilizing the carbon active sites,
364 which become less reactive for the oxidation reaction, as occurs when carbon materials
365 are doped with P [14, 17, 41, 45, 47]. Nevertheless, they could also act as a physical
366 barrier, blocking the access of oxygen to the active sites.

367 To investigate the oxidation evolution of the carbon surface, the activated carbons
368 were oxidized in air at different temperatures (between 120-350 °C) for 2 h and then
369 characterized in situ by TPD. It is interesting to mention that ACP2800 was highly
370 resistant to gasification in air, with no significant weight loss observed at 350 °C for 2 h.
371 However, the air oxidation of ACG800 at 350 °C for 2 h produced a carbon burn-off of
372 about 11 wt. %. Figure 3 shows the resulting CO and CO₂ evolution profiles during the
373 TPD of the oxidized samples at different temperatures. The TPD results evidence that
374 oxidation of the phosphoric acid-activated carbon (ACP2800) at temperatures lower
375 than 300 °C increases only the amount of CO evolved at about 860 °C, accompanied by
376 a small evolution of CO₂ at the same temperature, suggesting that oxidation of the
377 carbon surface at temperatures lower than 300 °C takes place through the oxidation of
378 C–P surface bonds, generating C–O–P bonds that are thermally stable up to 700 °C. At
379 higher oxidation temperatures (325 and 350 °C), the evolution of CO (and CO₂) during
380 the TPD experiments at high temperature (860 °C) seems to keep constant, which
381 suggests that the surface P groups are completely oxidized and other oxygen surface

382 complexes, thermally less stable, are formed, decomposing as CO and CO₂ at lower
383 temperatures (~700 °C for CO and ~500 and 700 °C for CO₂).

384 Oxidation of ACG800 activated carbon that contains no P surface groups
385 (especially at low oxidation temperatures, <300 °C) causes a more pronounced increase
386 in the evolution of CO (and CO₂) at lower temperatures (~700 °C for CO and ~500 and
387 700 °C for CO₂), compared to that of ACP2800, indicating that oxidation of this sample
388 takes place preferentially on the carbon surface, generating OSG of lower thermal
389 stability. Two broad peaks are found in the CO₂ profiles of ACG800 oxidized samples
390 (Figures 3d). The low temperature peak (c.a. 500 °C) could be attributed to
391 decomposition of lactone groups and the higher temperature peak (c.a. 700 °C) can be
392 originated from the more stable anhydride groups. In the case of ACP2800 oxidized
393 samples, in addition to these two broad peaks another sharp peak is observed at 860 °C
394 that can be associated to decomposition of stable O=C–O–P surface groups, as already
395 mentioned in Section 3.1. Oxidation at low temperature seems to preferentially form
396 lactone type groups on the surface of ACG800 and anhydride ones on the surface of
397 ACP2800, increasing the amount of both surface oxygen groups with oxidation
398 temperature, especially for ACG800, which is a typical behavior, previously observed
399 for other oxidized carbon materials [48, 49].

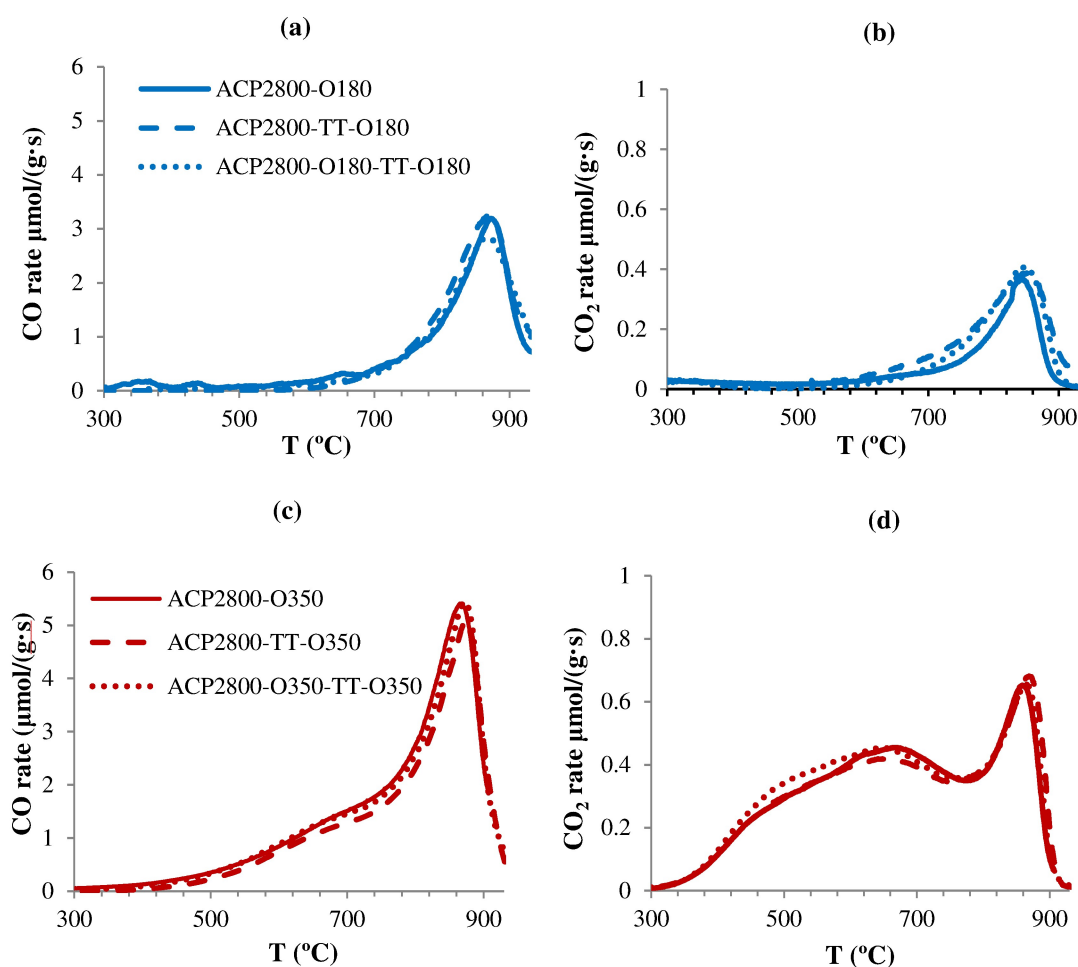


400

401 **Figure 3.** Amount of CO and CO₂ evolved as a function of temperature during the TPD
 402 experiments of ACP2800 (a and b, respectively) and ACG800 (c and d, respectively) after air
 403 oxidation at different temperatures (120, 180, 240, 300, 325 and 350 °C) for 2h.

404 To elucidate the chemical nature and stability of P in phosphorus-containing
 405 activated carbons, reduction and re-oxidation of these (P) surface groups has been
 406 studied after subjecting ACP2800 carbon to successive thermal treatments in N₂
 407 atmosphere up to 900 °C (-TT) and under air oxidations at 180 and at 350 °C for 2h (-
 408 O180 or -O350). TPD profiles of ACP2800 sample subjected to these successive
 409 treatments are shown in Figure 4. The TPD profile of the sample ACP2800 previously
 410 thermal treated in inert atmosphere up to 900 °C, followed by in-situ oxidation in air at
 411 180 °C for 2 h (ACP2800-TT-O180) overlaps with that for ACP2800-O180, showing
 412 that the same OSG (decomposing as CO and CO₂) were formed (Figure 4a and b). In a

413 second experiment, ACP2800 was previously subjected to air oxidation at 180 °C, then,
414 it was thermal treated in inert atmosphere at 900 °C and, finally, it was air oxidized
415 again at 180 °C. The TPD profile of this sample, ACP2800-O180-TT-O180, also
416 coincides with that of the previous ones. These results evidence that the P surface
417 complexes of this carbon can be reduced and oxidized again and that this behavior is
418 completely reversible, despite the fact that during the reduction/oxidation cycles slight
419 gasification of the carbon surface takes place through the evolution of CO/CO₂ during
420 the TPD experiments (with a total carbon burn-off of 3.1 ± 0.3 wt. %). After the thermal
421 treatment in inert atmosphere, the new surface sites generated by CO (and CO₂) release
422 (probably of C'-P type) seem to react with oxygen when exposed to air to (re)generate
423 (again) the oxygen-phosphorus (C'-O-P) surface groups. This behavior indicates that
424 oxidation takes place initially on the C-P bonds oxidizing them to C-O-P and that this
425 system is reversible upon heat treatment to high temperature, evidencing a redox
426 character. No loss of surface P was observed (by XPS and ICP-OES) after the different
427 reduction/oxidation cycles. This redox character seems to affect also to the other formed
428 oxygen surface groups, less thermally stable, in the case that the oxidation temperature
429 is higher than 300 °C (see Figures 4c and d for an oxidation temperature of 350 °C). The
430 carbon burn-off caused during the TPD experiment for ACP2800 oxidized at 350 °C
431 (ACP2800-O350-TT) was of 7.7 ± 0.5 wt. %.



432

433 **Figure 4.** Amount of CO and CO₂ evolved as a function of temperature during the TPD
 434 experiment for ACP2800 subjected to oxidations in air at 180 °C (-O180°C) (a and b,
 435 respectively) and 350 °C (-O350C) (c and d, respectively) and thermal treatments in inert
 436 atmosphere at 900 °C (-TT).

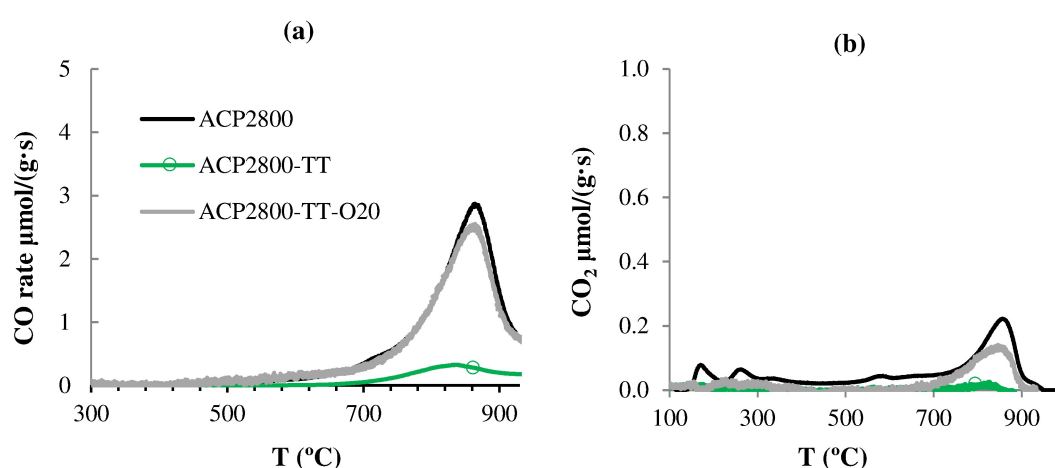
437

438 It is well known that the carbon surface heat treated at high temperatures in N₂ is
 439 not stable and may re-adsorb oxygen even at room temperature [50]. Re-oxidation of the
 440 phosphoric acid activated carbons at room temperature after being heat treated at high
 441 temperature (>860 °C) may also take place during air storage taking into account the
 442 high concentration of free sites, highly reactive and susceptible to be re-oxidized. In
 443 fact, after the TPD analysis the ACP2800 carbon showed a self-heating effect upon
 444 contact with air after cooling down to room temperature, also observed by others
 445 authors [11]. Figure S2 displays a thermogravimetric and differential thermal analysis

446 (TG-DTA) of ACP2800 subjected firstly to a thermal treatment in N₂ up to 900 °C and
447 later, once the sample is cooling down to room temperature under N₂ flow, to an air-
448 oxidation step at 25 °C for 120 min. During the thermal treatment, the TGA curve
449 exhibits two distinct weight loss steps and the DTA curve shows two endothermic
450 peaks. The first weight loss step in the temperature range of 25-100 °C, which was
451 accompanied by an endothermic peak in the DTA curve, is due to the loss of residual
452 water in the carbon. The second weight loss step in the temperature range of 700-800
453 °C, which was accompanied by an endothermic peak around 800 °C in the DTA curve,
454 corresponds to the decomposition of C–O–P type bonds in agreement with the TPD
455 results (Figure 2a). The introduction of air at 25°C, in the last step of the experiment,
456 leads to a sharp exothermic peak in the DTA curve (+6 °C) and a weight increment of
457 3.0 % in the TGA curve. Thus, it is suggested that new C'-O-PO₃ groups could be
458 generated on heat-treated samples in inert atmosphere after exposure to air and storage
459 at room temperature. For this reason, ACP2800 subjected to a thermal treatment in
460 nitrogen at 900 °C was exposed to air flow at 20 °C for 2h. This sample was denoted as
461 ACP2800-TT-O20. Figure 5 shows the CO and CO₂ TPD profiles for ACP2800-TT-
462 O20. As a baseline, the TPD for ACP2800-TT without exposure to air flow is also
463 presented. The TPD results for ACP2800-TT-O20 evidence mainly desorption of CO at
464 high temperatures in the same temperature range as that observed for the original
465 activated carbon and for the oxidized sample at temperatures lower than 300 °C,
466 confirming the oxidation of the C'-P type groups to C'-O-P ones (their (re)generation),
467 even by oxidation at room temperature. The weight gain observed in the initial step of
468 the oxidation profile of ACP2800-TT (Figure S2, TG-DTA curve) correlates quite well
469 with the total amount of oxygen gained by ACP2800-TT-O20, 3.1 wt. %, calculated
470 from the total CO and CO₂ evolved during the TPD (Figure 5).

471 3.3. Characterization of the treated activated carbons

472 P_{2p} spectra of ACP2800 and the corresponding treated samples are presented in
473 Figure S3. As a general observation, it can be stated that there are not big differences
474 among the P_{2p} spectra for the different samples, despite the fact that ACP2800 has been
475 treated in very drastic different ways (air oxidation at 350 °C for 2 hours and thermal
476 treatment in inert atmosphere at 900 °C). After oxidation of ACP2800 at 350 °C for 2 h
477 (ACP2800-O350) the P_{2p} peak shows a slight displacement to higher binding energies,
478 which can be associated to the presence of few more polyphosphates groups, of C-O-
479 PO_3 , $(CO)_2PO_2$ and $(CO)_3PO$ types, on the surface of the carbon. On the other hand, the
480 thermally treated samples in inert atmosphere (-TT) should present a shift of the binding
481 energy of the maximum of the P_{2p} peak to lower binding energies compared to that for
482 ACP2800 (and for that of ACP2800-TT-O350), showing a reduction of the most
483 oxygenated P groups (C-O-P type) to C- PO_3 , C_2PO_2 and/or C_3PO type. However, the
484 peaks are positioned at the same binding energies as that of the fresh activated carbon,
485 confirming that re-oxidation of the C- PO_3 type groups takes place once the samples are
486 exposed to ambient air, before XPS analysis.



487

488 **Figure 5.** Amount of CO (a) and CO₂ (b) evolved as a function of temperature during the TPD
489 of ACP2800 and ACP2800-TT without exposure to air and that of ACP2800 submitted to a
490 thermal treatment at 900° C, followed by oxidation in air at 20 °C for 1 h (ACP2800-TT-O20).

491 These results would explain the unexpectedly and large amount of oxygen left in all
492 phosphoric acid activated carbons prepared or heated at high temperatures in inert
493 atmosphere reported in the literature [8, 11, 12, 14]. In those cases, the oxygen content
494 measurement was carried out by elemental analysis, FTIR, XPS, etc., in which the
495 samples had been exposed to ambient air before the analysis. These results also support
496 that the more thermally stable groups seem to be C-PO₃ ones, which are very reactive
497 and can be re-oxidized to C-O-PO₃ type groups, even at room temperature, upon contact
498 with air. Therefore, the surface chemistry of these thermally treated carbons could
499 change during different storage conditions.

500 Table 3 presents the total amounts of CO and CO₂ released from the carbon
501 samples during the TPD experiments, obtained by integration the areas under the TPD
502 peaks, and the C, O, and P surface concentrations measured by XPS for the treated
503 samples with their uncertainties (see Figure S3). The results obtained for ACP2800 and
504 the derived carbons reveal very similar surface P content that is even slightly higher
505 after the different treatments, confirming the high stability of these surface P complexes
506 generated after the chemical activation of olive stone with H₃PO₄ at 800 °C. It has to be
507 mentioned that the N₂ adsorption-desorption and the CO₂ adsorption results (Table S1)
508 do not show relevant differences in the porous texture of the treated samples when they
509 are compared to those of the fresh activated carbon, indicating that the slight partial
510 gasification of the ACP2800 carbon during the different oxidation/reduction treatment
511 did not modify the porous texture and specific surface area of this carbon.

512

513 **Table 3.** Amount of CO and CO₂ evolved from the original and treated activated carbons and
 514 the surface chemistry characterization (XPS): total and surface oxygen concentrations. The
 515 uncertainties are discussed in the text and are provided in parentheses.

Sample	TPD				XPS (%wt)			
	CO ($\mu\text{mol/g}$)	CO ₂ ($\mu\text{mol/g}$)	O(TPD) ^a % wt	O-P(TPD) ^b % wt	C1s	P2p	O1s(XPS) ^c	O-P(XPS) ^d
AG800	305 (6)	652 (5)	2.6 (0.2)	n.a.	96.8 (0.8)	0.0 (0.1)	3.2 (0.2)	n.a.
ACG800-O350	3179 (8)	1455 (8)	9.7 (0.6)	n.a.	89.7 (0.7)	0.0 (0.1)	9.9 (0.4)	n.a.
ACG800-TT	164 (3)	22 (1)	0.3 ^e (0.1)	n.a.	95.6 (0.8)	0.3 (0.1)	3.5 (0.3)	n.a.
ACP2800	2735 (7)	305 (3)	5.4 (0.4)	4.1 (0.4)	87.3 (0.6)	3.5 (0.2)	9.2 (0.3)	5.0 (0.3)
ACP2800-O350	5139 (9)	1321 (7)	12.5 (0.7)	5.6 (0.7)	82.8 (0.6)	3.8 (0.3)	12.8 (0.4)	5.8 (0.3)
ACP2800-TT	507 (6)	112 (2)	1.2 ^e (0.2)	1.1 ^e (0.2)	89.6 (0.6)	3.6 (0.2)	6.5 (0.3)	4.6 (0.2)
ACP2800-TT-O20	2450 (7)	111 (3)	4.3 (0.2)	3.1 (0.2)	89.4 (0.7)	3.7 (0.3)	6.6 (0.3)	4.7 (0.2)
ACP2800-TT-O350	5107 (8)	1182 (8)	12.0 (0.7)	5.8 (0.7)	85.3 (0.6)	4.0 (0.3)	10.4 (0.4)	6.0 (0.3)

516 ^a Total oxygen from the total amounts of CO and CO₂ evolved

517 ^b Total oxygen bonded to P (as C-O-P) from the amounts of CO and CO₂ evolved at 860 °C.

518 ^c Surface oxygen content from XPS measurements. The samples were exposed to ambient air.

519 ^d Surface oxygen bonded to P from XPS = P·(4·COPO₃+3·CPO₃+C₃PO)

520 ^e not exposed to ambient air

521 n.a.: not applicable

522 From the amount of CO and CO₂ evolved during the TPD experiments, the total
 523 oxygen content, O(TPD), was calculated and compared to the surface oxygen content
 524 obtained from XPS analysis, O(XPS) (Table 3). Papier *et al.* [51] indicated that the 80-
 525 90 % peak area of the O1s peak represents the contribution of surface atoms, or atoms
 526 of the 3.5-4 nm thick outer shell of the particle. However, TPD results reveal also
 527 oxygen-containing groups located on the surface of meso- or/and micropores, deeper in
 528 the carbon particle. The amount of oxygen bonded to P on the activated carbon prepared
 529 by chemical activation and the corresponding derived carbons has also been calculated
 530 taking into account both characterization techniques: i) from deconvolution of the TPD
 531 profile, quantifying the peak evolved at 860 °C (O-P(TPD)) and ii) from the amount of
 532 the different surface P species obtained from deconvolution of the P2p spectra (O-
 533 P(XPS)). From the TPD results, the total amount of oxygen (from total CO and CO₂
 534 evolved) and that bonded to a P group (C-O-P) can be quantified, since the P type
 535 groups seem to decompose to CO (and CO₂) at 860 °C, as it was previously indicated. It

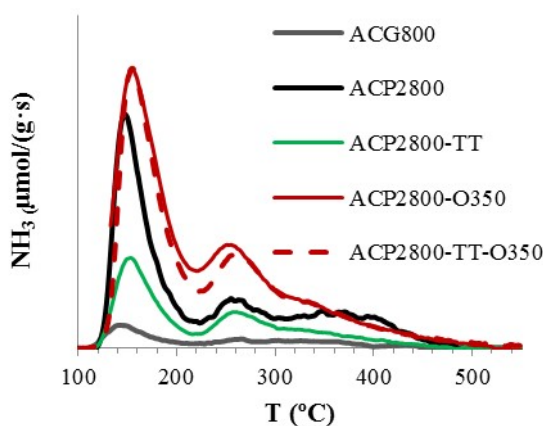
536 is remarkable to note the low uncertainties obtained which represent the 95 %
537 confidence interval calculated from three replicate measurements, evidencing the
538 reproducibility of the TPD and XPS measurements.

539 The observed general trend for oxygen surface content on ACG800 and ACP2800
540 and their corresponding derived carbons was predictable, being lower after the thermal
541 treatment and higher after the oxidation process. However, certain differences can be
542 appreciated between these two carbons. Similar values of O(XPS) and O(TPD) for the
543 fresh ACG800 activated carbon can be observed, indicating a homogeneous distribution
544 of oxygen surface groups on the whole particle surface. On the other hand, the high
545 value of O(XPS) compared to that obtained from TPD, O(TPD), for ACP2800 could
546 indicate that a higher proportion of oxygen groups could be concentrated on the external
547 surface of the carbon particles. However, it has to be pointed out that (and contrary to
548 ACG800 sample) not all the oxygen surface content of this sample is being taking into
549 account during the first TPD experiment, as was shown in Figures 3a. In this sense, the
550 O(TPD) value observed for ACP2800 after the thermal treatment (ACP2800-TT) of 1.2
551 ± 0.2 wt.% represents about 22 % of that for the fresh carbon (O(TPD) = 5.4 ± 0.4
552 wt.%) and this surface oxygen seems to be attached to surface P, given that the value of
553 1.1 wt. % of O-P(TPD) for this sample represent about 90 % of the O(TPD) value.
554 Furthermore, the high values of O-P(XPS) and O-P(TPD) observed for ACP2800 and
555 its derived carbons prepared by oxidation at temperatures lower than 300 °C, very
556 similar to their respective total XPS and TPD oxygen amount, indicate that most of the
557 oxygen present in the carbon particles seems to be bonded to surface P. Once ACP2800
558 is oxidized at higher temperature (350 °C) the total amount is much higher than that
559 referred to O-P because, apart from oxidation of C-P to C-O-P bonds, oxidation of the

560 carbon surface takes place, generating oxygen surface groups of lower thermal stability
561 that decompose as CO at lower temperatures in the DTP.

562 The NH₃-TPD profiles for ACG800, ACP2800, ACP2800-TT, ACP2800-O350 and
563 ACP2800-TT-O350 samples after adsorption and desorption of NH₃ at 100 °C are
564 compared in Figure 6. ACG800 sample presents an almost negligible desorption of
565 NH₃. On the other hand, the NH₃ desorption profile of ACP2800 shows two maxima, at
566 around 150 and 250 °C. The first one is known to arise from desorption of weakly
567 adsorbed NH₃ molecules (probably by hydrogen-bonded), identified on zeolite supports
568 [52]. However, it can also be related to weak acidic groups of C-O-PO₃ type on these
569 carbon materials since ACP2800, which desorbs a higher amount of NH₃ at this
570 temperatures compared to that of ACP2800-TT, presented a higher amount of oxygen-
571 containing P groups of C-O-PO₃ type, as was showed in Figure 2a. ACP2800-TT was
572 not exposed to ambient air before the adsorption of NH₃. This sample desorbed a small
573 amount of CO (and CO₂) at high temperatures in the TPDs experiments (Figures 2a),
574 associated to decomposition of C-O-PO₃ groups, which suggest the presence of a
575 relatively high amount of surface groups of C₂PO₂ and/or C₃PO type, instead of C-
576 OPO₃ one, that may contribute to the low acidity of this sample. On the other hand, the
577 shoulder at 250 °C and the large tail at higher temperatures may originate from NH₃
578 adsorbed on strong Brønsted acid sites [33]. The acidity of this type is related mainly to
579 the high amount of P retained on the carbon surface and probably associated to OH in
580 the phosphates groups. The total surface acidity for ACP2800 increases after air
581 oxidation at 350 °C, given that a high amount of oxygen-containing P groups of C-O-
582 PO₃ type are formed, as was deduced from results reported in Figures 3a and b and in
583 Table 3. Finally, the similar NH₃-TPD profiles obtained for ACP2800-O350 and
584 ACP2800-TT-O350 samples also confirm the (re-)oxidation of the P surface groups (C-

585 P to C-O-P types) after the thermal treatment in inert atmosphere and the acid character
586 of these oxygen-containing P groups.



587
588 **Figure 6.** NH₃-TPD profiles of the activated carbons ACG800, ACP2800, ACP2800-TT,
589 ACP2800-O350 and ACP2800-TT-O350 after NH₃ adsorption/desorption at 100 °C.

590

591 Scheme 1 represents some of the possible P surface groups formed during
592 phosphoric acid activated carbons surface reduction and oxidation reactions. Activated
593 carbons prepared by chemical activation of lignocellulosic materials with phosphoric
594 acid at temperatures below 600 °C have been reported to present mainly oxygen-
595 containing P surface groups of type C-O-PO₃ (Scheme 1a) [7, 8, 19, 33]. Dehydration of
596 P-OH groups of these surface P complexes (from 600 to 750° C) and aromatic
597 condensation of the carbon substrate at higher temperatures seem to be responsible of
598 the formation of H₂O and H₂, respectively, in the gas phase and new C-P bonds on the
599 carbon surface. The C-O-P bonds are thermally very stable and decompose only at
600 temperatures higher than 700 °C, producing CO (and CO₂) in the gas phase and C'-P
601 bonds (that may include C'PO₃, C'₂PO₂ (Scheme 1b) and C'₃PO (Scheme 1c) surface
602 groups, depending on the activation/oxidation treatment and temperature). The C₃PO
603 groups seem to be very stable even at 1000 °C, given that the P content on the surface of
604 these carbons remains constant or slightly increases after the thermal treatment at this

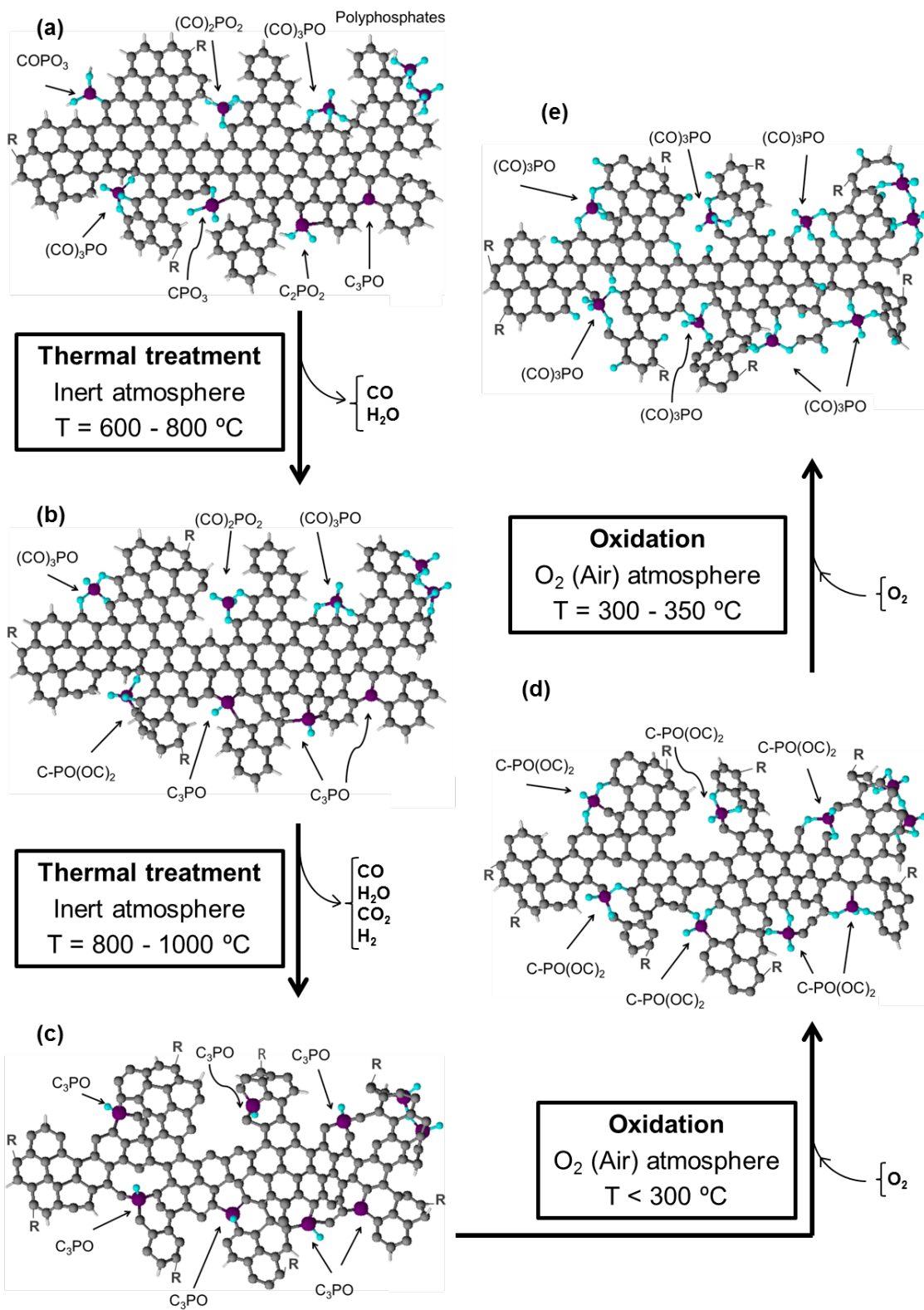
605 temperature (see Table 3). Oxidation of the carbon surface after being treated in N₂ at
606 1000° C (i.e., with all the P-surface group being converted in C₃PO) with molecular
607 oxygen at temperatures lower than 300 °C seems to take place only through the C–P
608 bond producing C–O–P ones; i.e., regenerating C-O-P type surface groups that may
609 include C₂PO-O-C, C-PO(OC)₂ (Scheme 1d) and (CO)₃PO (Scheme 1e)), depending on
610 the intensity of the oxidation treatment (oxidation time and/or temperature). Only after
611 oxidation at temperatures higher than 300 °C, these C–O–P bonds become saturated (all
612 of them of (CO)₃PO type groups) and oxidation of the carbonaceous substrate seems to
613 be possible, with production of oxygen surface groups that although are less stable than
614 those of P type, still present a relatively high thermal stability, decomposing at
615 moderated temperatures (between 500 and 800 °C; see Fig. 2a). Formation of
616 polyphosphate type groups cannot be disregarded on the surface of these carbons.

617 The surface of these activated carbons with oxygen-containing P groups should be a
618 strong acceptor of spill-over oxygen [53, 54]. The formation of these oxygen surface
619 groups on the carbonaceous substrate that decompose at lower temperatures might be
620 explained by a spill-over mechanism, involving adsorbed oxygen on the P surface
621 groups and migration of activated oxygen species from these P surface complexes to the
622 carbonaceous substrate [54], increasing the rate of formation of these oxygen surface
623 groups of lower stability with oxidation temperature (>300 °C).

624 These results may explain the effect of P surface groups on the enhancement of
625 carbon oxidation resistance observed for many carbon-containing P materials (fibers,
626 composites, etc) [9, 14, 17, 41, 45-47]. ACP2800 carbon, despite having similar BET
627 surface area and higher mesopore volume than ACG800, is resistant to air oxidation up
628 to 550 °C, whereas ACG800 carbon starts to lose weight at about 350 °C (see the
629 thermogravimetric analysis profiles in air for these two activated carbons in Figure S4).

630 Thus, the presence of O bonded to both a carbon site and a P group seems to be the
631 critical factor for maintaining the carbon oxidation inhibition effect (by site blockage)
632 [14], given that although the C-P bond is very reactive to oxygen, even at room
633 temperature, the C-O-P group is thermally very stable and appears to be the preferential
634 (and the only) surface product upon oxidation of carbons with P surface groups, at least
635 until saturation of these P-surface group with oxygen. The loss of such oxygen (or its
636 connecting bond) seems to be very difficult at typical O₂ gasification/combustion
637 temperatures (300-700 °C), given that the C-O-P group does not decompose at
638 temperatures lower than 700 °C (and the high thermal stability of the C-P bond). A
639 possible oxygen spill-over mechanism, given rise to other C-oxygen groups of lower
640 stability on the surface of the carbonaceous substrate, once the oxidation of the P groups
641 is completed, may play an important role in reducing the oxidation inhibition at higher
642 temperatures. Polyphosphates surface groups (also possible on the surface of these
643 carbons) may function as both physical barrier and site blockers.

644 On the other hand, the fact that the C'-P bond generated at high temperature
645 treatment is easily oxidized to C'-O-P ones, even at 20 °C, would explain the high
646 oxygen content observed for activated carbons prepared by chemical activation of
647 lignocellulosic materials with H₃PO₄ at high temperatures (>700 °C). Moreover, the low
648 enough uncertainties obtained suggest that these results would also be applied to those
649 carbons prepared by the same experimental procedure at lower activation temperatures
650 and/or to those post-heat treated at high temperature in inert atmosphere and exposed to
651 ambient air [8, 11, 12, 14, 19, 46].



652

653 **Scheme 1.** Possible P surface groups formed during phosphoric acid activated carbons surface
 654 oxidation and reduction reactions. (Greys: C, purple: P, blue: O, silver: H; R represents other
 655 similar carbonaceous matrix structures).

656 **5. Conclusions**

657 Chemical activation of olive stone with phosphoric acid produces activated carbons
658 with high BET surface areas, compared to those of olive stone chars carbonized at
659 similar temperatures that are usually below 200 m²/g, and a relatively high content of P
660 surface groups that remain very stable on the carbon surface at high temperatures. TPD
661 and XPS results point out that these P surface groups preferentially reacts with oxygen,
662 prior to carbon gasification, through the oxidation of C–P bond, forming C–O–P ones,
663 which are thermally stable at temperatures lower than 700 °C. Thermal treatments at
664 higher temperature (about 860 °C) decompose the C-O-P type surface groups to less
665 oxygenated P groups on the carbon surface (of C-P type) generating CO (and CO₂) in
666 the gas phase. These C-P groups seem to be very reactive and are (re)oxidized upon
667 contact with air, even at room temperature, forming again C-O-P type groups. Thus, the
668 presence of these oxygen-containing P surface groups with an interesting redox
669 functionality of high chemical and thermal stability seems to be responsible of the high
670 oxygen content (once exposed to ambient air) and high oxidation resistance of this kind
671 of porous carbons.

672 **Acknowledgments**

673 We gratefully thank Spanish Ministry of Economy and Competitiveness (MINECO) and
674 FEDER (Projects CTQ2015-68654-R) for financial support. M.J.V.R. gratefully thanks
675 MINECO for a FPI fellowship (BES-2010-032213).

676 **References**

- 677 [1] J. Bedia, J.M. Rosas, J. Marquez, J. Rodriguez-Mirasol, T. Cordero, Preparation and
678 characterization of carbon based acid catalysts for the dehydration of 2-propanol,
679 Carbon, 47 (2009) 286-294.
680 [2] J. Bedia, J.M. Rosas, J. Rodriguez-Mirasol, T. Cordero, Pd supported on
681 mesoporous activated carbons with high oxidation resistance as catalysts for toluene
682 oxidation, Appl Catal B-Environ, 94 (2010) 8-18.

- 683 [3] J. Bedia, R. Ruiz-Rosas, J. Rodriguez-Mirasol, T. Cordero, Kinetic Study of the
684 Decomposition of 2-Butanol on Carbon-Based Acid Catalyst, *Aiche J*, 56 (2010) 1557-
685 1568.
- 686 [4] M.O. Guerrero-Perez, M.J. Valero-Romero, S. Hernandez, J.M.L. Nieto, J.
687 Rodriguez-Mirasol, T. Cordero, Lignocellulosic-derived mesoporous materials: An
688 answer to manufacturing non-expensive catalysts useful for the biorefinery processes,
689 *Catal Today*, 195 (2012) 155-161.
- 690 [5] K.G. Haw, W.A.W. Abu Bakar, R. Ali, J.F. Chong, A.A.A. Kadir, Catalytic
691 oxidative desulfurization of diesel utilizing hydrogen peroxide and functionalized-
692 activated carbon in a biphasic diesel-acetonitrile system, *Fuel Process Technol*, 91
693 (2010) 1105-1112.
- 694 [6] L.B. Khalil, B.S. Girgis, T.A.M. Tawfik, Decomposition of H₂O₂ on activated
695 carbon obtained from olive stones, *J Chem Technol Biot*, 76 (2001) 1132-1140.
- 696 [7] J.M. Rosas, J. Bedia, J. Rodriguez-Mirasol, T. Cordero, Preparation of hemp-
697 derived activated carbon monoliths. adsorption of water vapor, *Ind Eng Chem Res*, 47
698 (2008) 1288-1296.
- 699 [8] J.M. Rosas, J. Bedia, J. Rodriguez-Mirasol, T. Cordero, HEMP-derived activated
700 carbon fibers by chemical activation with phosphoric acid, *Fuel*, 88 (2009) 19-26.
- 701 [9] J.M. Rosas, R. Ruiz-Rosas, J. Rodriguez-Mirasol, T. Cordero, Kinetic study of the
702 oxidation resistance of phosphorus-containing activated carbons, *Carbon*, 50 (2012)
703 1523-1537.
- 704 [10] M.J. Valero-Romero, A. Cabrera-Molina, M.O. Guerrero-Perez, J. Rodriguez-
705 Mirasol, T. Cordero, Carbon materials as template for the preparation of mixed oxides
706 with controlled morphology and porous structure, *Catal Today*, 227 (2014) 233-241.
- 707 [11] A.M. Puziy, O.I. Poddubnaya, A. Martinez-Alonso, F. Suarez-Garcia, J.M.D.
708 Tascon, Surface chemistry of phosphorus-containing carbons of lignocellulosic origin,
709 *Carbon*, 43 (2005) 2857-2868.
- 710 [12] A.M. Puziy, O.I. Poddubnaya, R.P. Socha, J. Gurgul, M. Wisniewski, XPS and
711 NMR studies of phosphoric acid activated carbons, *Carbon*, 46 (2008) 2113-2123.
- 712 [13] A.M. Puziy, O.I. Poddubnaya, A.M. Ziatdinov, On the chemical structure of
713 phosphorus compounds in phosphoric acid-activated carbon, *Appl Surf Sci*, 252 (2006)
714 8036-8038.
- 715 [14] X.X. Wu, L.R. Radovic, Inhibition of catalytic oxidation of carbon/carbon
716 composites by phosphorus, *Carbon*, 44 (2006) 141-151.
- 717 [15] D.W. Mckee, C.L. Spiro, E.J. Lamby, The Inhibition of Graphite Oxidation by
718 Phosphorus Additives, *Carbon*, 22 (1984) 285-290.
- 719 [16] S.G. Oh, N.M. Rodriguez, In-Situ Electron-Microscopy Studies of the Inhibition of
720 Graphite Oxidation by Phosphorus, *J Mater Res*, 8 (1993) 2879-2888.
- 721 [17] Y.J. Lee, L.R. Radovic, Oxidation inhibition effects of phosphorus and boron in
722 different carbon fabrics, *Carbon*, 41 (2003) 1987-1997.
- 723 [18] J. Bedia, R. Barrionuevo, J. Rodriguez-Mirasol, T. Cordero, Ethanol dehydration to
724 ethylene on acid carbon catalysts, *Appl Catal B-Environ*, 103 (2011) 302-310.
- 725 [19] J.M.R. J.J. Ternero-Hidalgo, J. Palomo, M.J. Valero-Romero, J. Rodríguez-
726 Mirasol, T. Cordero, Functionalization of activated carbons by HNO₃ treatment:
727 Influence of phosphorus surface groups, *Carbon*, 101 (2016) 409-419.
- 728 [20] E. Gonzalez-Serrano, T. Cordero, J. Rodriguez-Mirasol, L. Cotoruelo, J.J.
729 Rodriguez, Removal of water pollutants with activated carbons prepared from H₃PO₄
730 activation of lignin from kraft black liquors, *Water Res*, 38 (2004) 3043-3050.

- 731 [21] J. Rodriguezmirasol, T. Cordero, J.J. Rodriguez, Co-2-Reactivity of Eucalyptus
732 Kraft Lignin Chars, Carbon, 31 (1993) 53-61.
- 733 [22] S. Brunauer, P.H. Emmett, E. Teller, Adsorption of gases in multimolecular layers,
734 J Am Chem Soc, 60 (1938) 309-319.
- 735 [23] M.M. Dubinin, E.D. Zaverina, L.V. Radushkevich, Sorbtsiya I Struktura
736 Aktivnykh Uglei .1. Issledovanie Adsorbtsii Organicheskikh Parov, Zh Fiz Khim+, 21
737 (1947) 1351-1362.
- 738 [24] K. Kaneko, C. Ishii, Superhigh Surface-Area Determination of Microporous Solids,
739 Colloid Surface, 67 (1992) 203-212.
- 740 [25] R.H. Dieck, Measurement Uncertainty: Methods and Applications, Fourth Edition;
741 ISA: Research Triangle Park, NC,, (2007) 277.
- 742 [26] T. Vernersson, P.R. Bonelli, E.G. Cerrella, A.L. Cukierman, Arundo donax cane as
743 a precursor for activated carbons preparation by phosphoric acid activation, Bioresource
744 Technol, 83 (2002) 95-104.
- 745 [27] M. Jagtoyen, F. Derbyshire, Activated carbons from yellow poplar and white oak
746 by H₃PO₄ activation, Carbon, 36 (1998) 1085-1097.
- 747 [28] F. Rodriguezreinoso, M. Molinasabio, M.T. Gonzalez, The Use of Steam and Co₂
748 as Activating Agents in the Preparation of Activated Carbons, Carbon, 33 (1995) 15-23.
- 749 [29] A.M. Puziy, O.I. Poddubnaya, A. Martinez-Alonso, F. Suarez-Garcia, J.M.D.
750 Tascon, Synthetic carbons activated with phosphoric acid III. Carbons prepared in air,
751 Carbon, 41 (2003) 1181-1191.
- 752 [30] H. Estrade-Szwarckopf, XPS photoemission in carbonaceous materials: A "defect"
753 peak beside the graphitic asymmetric peak, Carbon, 42 (2004) 1713-1721.
- 754 [31] S.W. Moulder JF, Sobol PE, Bomben K. In: Chastain J, editor, Handbook of X-ray
755 photoelectron spectroscopy. 2nd ed. Eden Prairie, MN: Perkin-Elmer Corporation,
756 Physical Electronics Division, (1992) 216-232.
- 757 [32] S.M. Briggs D, Practical Surface Analysis, Auger and X-ray Photoelectron
758 Spectroscopy, Wiley, Chichester, UK, 1 (1990).
- 759 [33] J. Bedia, R. Ruiz-Rosas, J. Rodriguez-Mirasol, T. Cordero, A kinetic study of 2-
760 propanol dehydration on carbon acid catalysts, J Catal, 271 (2010) 33-42.
- 761 [34] S.W. Moulder JF, Sobol PE, Bomben KD, Handbook of X-ray Photoelectron
762 Spectroscopy, Physical Electronics Inc. Eden Prairie, (1995) 4872-4875.
- 763 [35] J. Bedia, J.M. Rosas, D. Vera, J. Rodriguez-Mirasol, T. Cordero, Isopropanol
764 decomposition on carbon based acid and basic catalysts, Catal Today, 158 (2010) 89-96.
- 765 [36] J.L. Figueiredo, M.F.R. Pereira, M.M.A. Freitas, J.J.M. Orfao, Modification of the
766 surface chemistry of activated carbons, Carbon, 37 (1999) 1379-1389.
- 767 [37] U. Zielke, K.J. Huttinger, W.P. Hoffman, Surface-oxidized carbon fibers .1.
768 Surface structure and chemistry, Carbon, 34 (1996) 983-998.
- 769 [38] B. Marchon, J. Carrazza, H. Heinemann, G.A. Somorjai, Tpd and Xps Studies of
770 O-2, Co₂, and H₂o Adsorption on Clean Polycrystalline Graphite, Carbon, 26 (1988)
771 507-514.
- 772 [39] C. Moreno-Castilla, F. Carrasco-Marin, F.J. Maldonado-Hodar, J. Rivera-Utrilla,
773 Effects of non-oxidant and oxidant acid treatments on the surface properties of an
774 activated carbon with very low ash content, Carbon, 36 (1998) 145-151.
- 775 [40] M.A. Montes-Moran, D. Suarez, J.A. Menendez, E. Fuente, On the nature of basic
776 sites on carbon surfaces: An overview, Carbon, 42 (2004) 1219-1225.
- 777 [41] W.M. Lu, D.D.L. Chung, Oxidation protection of carbon materials by acid
778 phosphate impregnation, Carbon, 40 (2002) 1249-1254.

779 [42] P.J. Hall, J.M. Calo, Secondary Interactions Upon Thermal-Desorption of Surface
780 Oxides from Coal Chars, *Energ Fuel*, 3 (1989) 370-376.

781 [43] G. Alberti, S. Cavalaglio, F. Marmottini, K. Mutusek, J. Megyeri, L. Szirtes,
782 Preparation of a composite gamma-zirconium phosphate silica with large specific
783 surface and its first characterisation as acid catalyst, *Appl Catal a-Gen*, 218 (2001) 219-
784 228.

785 [44] J.F. Vivo-Vilches, E. Bailon-Garcia, A.F. Perez-Cadenas, F. Carrasco-Marin, F.J.
786 Maldonado-Hodar, Tailoring the surface chemistry and porosity of activated carbons:
787 Evidence of reorganization and mobility of oxygenated surface groups, *Carbon*, 68
788 (2014) 520-530.

789 [45] S. Labruquere, R. Pailler, R. Naslain, B. Desbat, Oxidation inhibition of carbon
790 fibre preforms and C/C composites by H₃PO₄, *J Eur Ceram Soc*, 18 (1998) 1953-1960.

791 [46] R. Berenguer, R. Ruiz-Rosas, A. Gallardo, D. Cazorla-Amoros, E. Morallon, H.
792 Nishihara, T. Kyotani, J. Rodriguez-Mirasol, T. Cordero, Enhanced electro-oxidation
793 resistance of carbon electrodes induced by phosphorus surface groups, *Carbon*, 95
794 (2015) 681-689.

795 [47] M. Seredych, C.T. Wu, P. Brender, C.O. Ania, C. Vix-Guterl, T.J. Bandoz, Role
796 of phosphorus in carbon matrix in desulfurization of diesel fuel using adsorption
797 process, *Fuel*, 92 (2012) 318-326.

798 [48] V. Gomez-Serrano, F. Piriz-Almeida, C.J. Duran-Valle, J. Pastor-Villegas,
799 Formation of oxygen structures by air activation. A study by FT-IR spectroscopy,
800 *Carbon*, 37 (1999) 1517-1528.

801 [49] Y. Otake, R.G. Jenkins, Characterization of Oxygen-Containing Surface
802 Complexes Created on a Microporous Carbon by Air and Nitric-Acid Treatment,
803 *Carbon*, 31 (1993) 109-121.

804 [50] R.-U.J. Carrasco-Marín F, Joly J p and Moreno-Castilla C, Effects of ageing on the
805 oxygen surface complexes on fa oxidized activated carbon,
806 *Journal of the Chemical Society, Faraday Transactions*, 92 (1996) 2779-2782.

807 [51] E. Papirer, R. Lacroix, J.B. Donnet, G. Nanse, P. Fioux, Xps Study of the
808 Halogenation of Carbon-Black .I. Bromination, *Carbon*, 32 (1994) 1341-1358.

809 [52] N. Katada, H. Igi, J.H. Kim, M. Niwa, Determination of the acidic properties of
810 zeolite by theoretical analysis of temperature-programmed desorption of ammonia
811 based on adsorption equilibrium, *J Phys Chem B*, 101 (1997) 5969-5977.

812 [53] L.T. Weng, P. Ruiz, B. Delmon, Classification of the roles of oxides as catalysts
813 for selective oxidation of olefins, *Studies in Surface Science and Catalysis*, 72 (1992)
814 399-413.

815 [54] G. Mul, J.P.A. Neeft, F. Kapteijn, J.A. Moulijn, The formation of carbon surface
816 oxygen complexes by oxygen and ozone. The effect of transition metal oxides, *Carbon*,
817 36 (1998) 1269-1276.

818